The Prevalence of each CR3BP in the Approximation of the Bicircular model ⋆

Castelli Roberto *

* *IFIM, Universität Paderborn, Warburger Str. 100, 33098 Paderborn, Germany (e-mail: robertoc@math.upb.de).*

Abstract:
This talk concerns the role played by the planar Circular Restricted Three-Body problem in the approximation of the Bicircular model. The comparison between the differential equations governing the dynamics leads to the definition of *Region of Prevalence* where one restricted model provides the best approximation of the four-body model. According to this prevalence, the Patched Three-Body Problem approximation is used to design first guess trajectories for a spacecraft travelling under the Sun-Earth-Moon gravitational influence.

Keywords: Bicircular model, Coupled Restricted Three-Body Problem Approximation, Invariant manifolds, Poincaré section

INTRODUCTION

Starting from the work of Belbruno and Miller, (Belbruno and Miller (1993)) where the perturbation of the Sun has been shown to decrease the amount of fuel necessary for a Earth-to-Moon transfer, the Sun-Earth-Moon-Spacecraft restricted 4-body model has been commonly adopted to describe the Spacecraft motion.

One of the technique used to approximate the 4-body dynamics, or in general the n-body problem, is the coupled restricted three-body problem approximation: partial orbits from different restricted problems are connected into a single trajectory, yielding energy efficient transfers to the Moon (Koon et al. (2001)), interplanetary transfers (Dellnitz et al. (2006)) or very complicated itineraries (Gómez et al. (2004)).

The procedure requires the choice of a Poincaré section where the phase spaces of the two different models have to intersect: the analysis of the Poincaré maps of the invariant manifolds reduces the design of the trajectory to the selection of a point on the section. The Poincaré section plays also a role in the accuracy of the approximation of the undertaken dynamical system: indeed the encounter with the Poincaré section is the criteria for switching from the first to the second restricted three-body problem. In the mentioned works the Poincaré section is chosen *a priori* by the user in order to accomplish certain design constraints or to simplify the selection of the connection point and it usually consists in a hyperplane passing through one of the primaries or lying along one of the coordinated axis.

Although it has been shown that for design purpose the solutions in a simplified model like the CR3BP are very good approximations to real trajectories in the complicated and full system (Parker (2006)), this work deepens from a more theoretical point of view on the role played by the two restricted three-body problems in the approximation of the 4-body system.

The undertaken model considered here for the 4-body dynamics is the Bicircular model (BCP), Simó et al. (1995), while the two restricted problems are the Earth-Moon CR3BP and the Sun-(Earth+Moon) CR3BP, where, in the last case, the Sun and the Earth-Moon barycenter play the role of primaries. The comparison of the mentioned systems leads to the definition of *Regions of Prevalence* in the space where one of the restricted problems performs, at least locally, the best approximation of the Bicircular model and therefore it should be preferred in designing the trajectory.

Then, setting the Poincaré section according to this prevalence, the coupled CR3BP approximation is implemented to design low energy transfers leaving Lyapunov orbits in the Sun-Earth system and leading to the Moon's region.

The plan of the paper is the following. In the first section the CR3BP is briefly recalled and the equations of motion for the BCP in the inertial reference frame are written. Then, in section 2, the comparison between the BCP and each one of the restricted problems is performed: this analysis enables to define, in section 3, the regions of prevalence of the two restricted systems in the approximation of the 4-body model. Section 4 concerns the design of the transfer trajectory while section 5 deepens on the numeral scheme used to analyze the Poincaré maps and the selection of the connection points. Finally in the last section some of the results are discussed.

1. DYNAMICAL MODELS

Circular Restricted Three-Body problem

The CR3BP is a simplified case of the general Three-Body Problem and models the motion of a massless particle under the gravitational influence of two bodies, with

⋆ Work supported by the Marie Curie Actions Research and Training Network AstroNet

masses $M_1 < M_2$, that are revolving with constant angular velocity in circular orbit around their center of mass, see Szebehely (1967). In the following only the planar motion is considered.

In a rotating reference frame centered in the center of mass, where the units of measure are normalized so that the total mass, the distance between the primaries and their angular velocity are equal to 1, the primaries are fixed on the x-axis at positions $(-\mu, 0)$ and $(1-\mu, 0)$ while the motion $z(t) = x(t) + iy(t)$ of the massless particle evolves following the differential equation

$$\frac{d^2z}{dt^2} + 2i\frac{dz}{dt} - z = -\left[\frac{(1-\mu)(z+\mu)}{\| z+\mu \|^3} + \frac{\mu(z-(1-\mu))}{\| z-(1-\mu) \|^3}\right] \quad (1)$$

where $\mu = M_2/(M_1 + M_2)$ is the mass ratio.

In (x, y) components the equation of motion assumes the form

$$\ddot{x} - 2\dot{y} = \Omega_x \ , \qquad \ddot{y} + 2\dot{x} = \Omega_y$$

where $\Omega(x, y) = (x^2+y^2)/2+(1-\mu)/r_1+\mu/r_2+\mu(1-\mu)/2$ is the potential function. The subscripts of Ω denote the partial derivatives, while $r_{1,2}$ are the distances between the moving particle and the primaries. The advantage to study the dynamics in a rotating frame is that the system (1) is Hamiltonian and autonomous and admits a first integral called Jacobi constant

$$J(x, y, \dot{x}, \dot{y}) = -(\dot{x}^2 + \dot{y}^2) + 2\Omega(x, y) \ .$$

The potential Ω admits five critical points, the Lagrangian points $L_i, i = 1 \dots 5$, and represent equilibrium points for the vector field. The points $L_{4,5}$ correspond to equilateral triangle configurations, while the remaining are placed on the x-axis and correspond to collinear configurations of the masses. Of particular interest for mission design purpose are L_1 and L_2 and the periodic orbits surrounding them that play the role of gates in the Hill's region, see for instance Koon et al. (2000).

Bicircular model

The Bicircular model (BCP), see Cronin et al. (1964), consists in a restricted four-body problem where two of the primaries are rotating around their center of mass, which is meanwhile revolving together with the third mass around the barycenter of the complete system. The massless particle is moving under the gravitational influence of the primaries and does not affect their motion. It is assumed that the motion of the primaries, as like as the motion of the test particle are co-planar. The low eccentricity of the Earth's and Moon's orbit and the small inclination of the Moon's orbital plane, make the Bicircular a quite accurate model to describe the dynamics of a spacecraft in the Sun-Earth-Moon system; see for instance Yagasaki (2004) and Mingotti et al. (2009).

Referring to Fig. 1, let S, E, M be the positions of the three primaries, namely the Sun, the Earth and the Moon while B and O indicate the Earth-Moon barycenter and the total center of mass of the system. For a given time-space unit, let us define w_1 and w_2 the angular velocities respectively of the couple S and B around O and the couple E and M around B; L_S and L_M the distances $\overline{SB}$ and $\overline{EM}$; M_m, M_e, M_s the masses of the Moon, the Earth and the Sun and G the gravitational constant. Moreover let μ_s and μ_m be the mass ratios

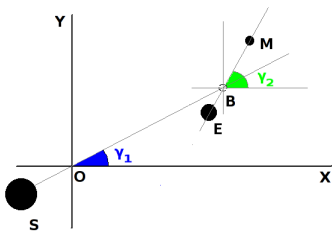

Fig. 1. Positions of the primaries in the inertial reference frame

$$\mu_m = \frac{M_m}{M_e + M_m}, \quad \mu_s = \frac{M_e + M_m}{M_e + M_m + M_s} \ . \quad (2)$$

With respect to an inertial reference frame (X, Y) whose origin is fixed in the barycenter O and where τ denotes the time coordinate, the positions of the primaries are given by

$$\begin{aligned} S &= -\mu_s L_S e^{i(\varphi_0 + w_1\tau)} \\ E &= (1-\mu_s) L_S e^{i(\varphi_0 + w_1\tau)} - \mu_m L_M e^{i(\phi_0 + w_2\tau)} \\ M &= (1-\mu_s) L_S e^{i(\varphi_0 + w_1\tau)} + (1-\mu_m) L_M e^{i(\phi_0 + w_2\tau)} \ . \end{aligned}$$

In order to lighten the notation, in the following $\gamma_1(\tau) = \varphi_0 + w_1\tau$ and $\gamma_2(\tau) = \phi_0 + w_2\tau$ are used.

The motion $Z(\tau) = X(\tau) + iY(\tau)$ of the spacecraft is governed by the second order differential equation

$$\frac{d^2Z}{d\tau^2} = -G\left[\frac{M_s(Z-S)}{\| Z-S \|^3} + \frac{M_e(Z-E)}{\| Z-E \|^3} + \frac{M_m(Z-M)}{\| Z-M \|^3}\right] \quad (3)$$

In the following sections the BCP is compared with two different restricted three-body problems: the CR3BP$_{EM}$ and the CR3BP$_{SE}$ where the Sun and the barycenter B with mass $M_b = M_e + M_m$ play the role of primaries. Three different reference frames and different units of measure are involved in the analysis: the inertial reference frame and the SE-synodical reference frame whose origin is set in the center of mass O and the EM-synodical reference frame centered in the point B.

Change of coordinates

Following the notation previously adopted, let (X, Y, τ) be the space-time coordinates in the inertial reference frame and the small letters (x, y, t) the coordinates in the rotating systems. When necessary, in order to avoid any ambiguity, the subscript (x_s, y_s, t_s) and (x_m, y_m, t_m) are used to distinguish the set of coordinates in the CR3BP$_{SE}$ and in the CR3BP$_{EM}$ respectively. In complex notation

$$Z := X + iY, \qquad z_m := x_m + iy_m, \qquad z_s := x_s + iy_s$$

the relations between the inertial and the synodical coordinates are given by

$$Z = L_S z_s e^{i\gamma_1}, \qquad \tau = \frac{t_s}{w_1}$$

$$Z = (1-\mu_s) L_S e^{i\gamma_1} + L_M z_m e^{i\gamma_2}, \qquad \tau = \frac{t_m}{w_2} \ .$$

Concerning with the two synodical systems, the relation between the time coordinates t_s and t_m is easily derived

$$t_s = \frac{w_1}{w_2} t_m$$

while the transformation between the space coordinates (x_s, y_s) and (x_m, y_m) depends on the mutual position of the primaries. Let θ be the angle between the positive x_s-semiaxis and the positive x_m-semiaxis:

$$\theta(\tau) := \gamma_2 - \gamma_1 = \theta_0 + (w_2 - w_1)\tau \ .$$

For any value of θ, the position and the velocity of a particle in the two different synodical systems satisfy the relations

$$z_m = \frac{L_S}{L_M} e^{-i\theta}\Big(z_s - (1-\mu_s)\Big)$$
$$\frac{dz_m}{dt_m} = \frac{L_S}{L_M}\frac{w_1}{w_2} e^{-i\theta}\Big[i\Big(1-\frac{w_2}{w_1}\Big)(z_s-(1-\mu_s)) + \frac{dz_s}{dt_s}\Big] \quad (4)$$

and

$$z_s = \frac{L_M}{L_S} e^{i\theta} z_m + (1-\mu_s)$$
$$\frac{dz_s}{dt_s} = \frac{L_M}{L_S}\frac{w_2}{w_1} e^{i\theta}\Big[i\Big(1-\frac{w_1}{w_2}\Big)(z_m) + \frac{dz_m}{dt_m}\Big] .$$

A second integration provides the relations between the accelerations in the two systems:

$$\frac{d^2 z_s}{dt_s^2} = \frac{L_M}{L_S}\left(\frac{w_2}{w_1}\right)^2 e^{i\theta}\cdot \Big[-\Big(1-\frac{w_1}{w_2}\Big)^2 z_m + 2i\Big(1-\frac{w_1}{w_2}\Big)\frac{dz_m}{dt_m} + \frac{d^2 z_m}{dt_m^2}\Big] . \quad (5)$$

The following equalities are consequence of the third Kepler's law

$$w_1^2 L_S^3 = G(M_s + M_e + M_m),\ w_2^2 L_M^3 = G(M_e + M_m) . \quad (6)$$

In this work the physical parameters adopted in the numerical simulations are set according with the Jet Propulsion Laboratory ephemeris (available on-line at http://ssd.jpl.nasa.gov/?constants). In particular the mass ratios are

$$\mu_s = 3.040423402066 \cdot 10^{-6}, \quad \mu_m = 0.012150581$$

being the masses of the bodies

$$M_s = 1.988924 \cdot 10^{30} \text{ kg} \quad M_e = 5.973712 \cdot 10^{24} \text{ kg}$$
$$M_m = 7.347686 \cdot 10^{22} \text{ kg} .$$

In the inertial reference frame, where the space coordinates are expressed in km and the time in seconds, the distances L_S and L_M are equal to

$$L_S = 149597870 \text{ km}, \ L_M = 384400 \text{ km}$$

while the values of the angular velocities w_1 and w_2 are

$$w_1 = 1.99098898 \cdot 10^{-7} \frac{\text{rad}}{\text{s}}, \ w_2 = 2.6653174179 \cdot 10^{-6} \frac{\text{rad}}{\text{s}} .$$

2. THE COMPARISON OF THE BCP WITH THE CR3BPS

The distance between the Bicircular model and each one of the CR3BP is estimated as the norm of the difference of the differential equations governing their dynamics, once they are written in the same reference frame and in the same units of measure. The comparison is performed in the synodical frame proper of the considered restricted problem, while the units of measure in both the cases will be the dimensional one.

Comparison with SE-CR3BP

To write the equation of motion for the BCP in SE-synodical coordinates without any time-space units rescale, only a rotation has to be applied to the inertial coordinates: $Z = \bar{z}e^{i\gamma_1}$, where $\bar{z} = z_s L_S$. In this setting the positions of the primaries are given by

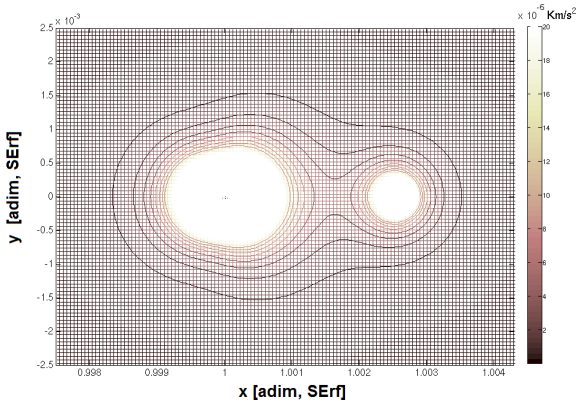

Fig. 2. Level curves of Δ_{SE} for $\theta = 0$

$$\bar{S} = -\mu_s L_S$$
$$\bar{E} = (1-\mu_s)L_S - \mu_m L_M e^{i(\gamma_2-\gamma_1)}$$
$$\bar{M} = (1-\mu_s)L_S + (1-\mu_m)L_M e^{i(\gamma_2-\gamma_1)} .$$

The double derivative of $Z(\tau)$ turns into

$$\frac{d^2 Z}{d\tau^2} = \left(\frac{d^2\bar{z}}{d\tau^2} + 2iw_1\frac{d\bar{z}}{d\tau} - w_1^2\bar{z}\right)e^{i\gamma_1}$$

then, substituting the new variables into (3), we infer

$$\frac{d^2\bar{z}}{d\tau^2} + 2iw_1\frac{d\bar{z}}{d\tau} - w_1^2\bar{z} = -G\Big[\frac{M_s(\bar{z}-\bar{S})}{\| \bar{z}-\bar{S} \|^3} + \frac{M_e(\bar{z}-\bar{T})}{\| \bar{z}-\bar{E} \|^3} + \frac{M_m(\bar{z}-\bar{M})}{\| \bar{z}-\bar{M} \|^3}\Big] . \quad (7)$$

In the same time-space frame, CR3BP$_{SE}$ is described by

$$\frac{d^2\bar{z}}{d\tau^2} + 2iw_1\frac{d\bar{z}}{d\tau} - w_1^2\bar{z} = -G\left[\frac{M_s(\bar{z}-\bar{S})}{\| \bar{z}-\bar{S} \|^3} + \frac{M_b(\bar{z}-\bar{B})}{\| \bar{z}-\bar{B} \|^3}\right] .$$

It follows the difference between the two models

$$\Delta_{SE}(\bar{z}) = \| BCP - CR3BP_{SE} \|$$
$$= G\Big|\Big| - \frac{M_e(\bar{z}-\bar{E})}{\| \bar{z}-\bar{E} \|^3} - \frac{M_m(\bar{z}-\bar{M})}{\| \bar{z}-\bar{M} \|^3} + \frac{M_b(\bar{z}-\bar{B})}{\| \bar{z}-\bar{B} \|^3}\Big|\Big| .$$

The gap between the two models arises from the fact that in the restricted three-body problem the Earth-Moon system is considered as a unique body concentrated in its center of mass instead of a binary system.

The distance between the two systems rapidly decreases to zero as the evaluation point is out of two disks around the primaries. For any different mutual position of the three primaries the picture of Δ_{SE} is different but self-similar up to rotation around the point B; in Fig. 2 the value of Δ_{SE} is plotted for $\theta = 0$.

Comparison with EM-CR3BP

Following the same procedure as before, the distance between the CR3BP$_{EM}$ and the BCP is achieved. Again, let $\bar{z}$ be used to denote the complex coordinates in a rotating reference frame and dimensional units of measure. Reminding that the origin of the EM-synodical frame is in the barycenter B that is revolving around the center of mass O, the inertial coordinate Z and $\bar{z}$ are linked by the formula

$$Z = B + \bar{z}e^{i\gamma_2} , \qquad B = (1-\mu_s)L_S e^{i\gamma_1} .$$

The positions of the primaries

$$\bar{S} = (S-B)e^{-i\gamma_2} = -L_S e^{i(\gamma_1-\gamma_2)}$$
$$\bar{E} = (E-B)e^{-i\gamma_2} = -\mu_m L_M$$
$$\bar{M} = (M-B)e^{-i\gamma_2} = (1-\mu_m)L_M$$

and the acceleration of the particle

$$\frac{d^2Z}{d\tau^2} = \left(\frac{d^2\bar{z}}{d\tau^2} + 2iw_2\frac{d\bar{z}}{d\tau} - w_2^2\bar{z} - w_1^2(1-\mu_s)L_S e^{i(\gamma_1-\gamma_2)}\right)e^{i\gamma_2}$$

give the differential equation for the BCP in dimensional EM-synodical coordinates

$$\frac{d^2\bar{z}}{d\tau^2} + 2iw_2\frac{d\bar{z}}{d\tau} - w_2^2\bar{z} - w_1^2(1-\mu_s)L_S e^{i(\gamma_1-\gamma_2)} = -G\left[\frac{M_s(\bar{z}-\bar{S})}{\| \bar{z}-\bar{S} \|^3} + \frac{M_e(\bar{z}-\bar{E})}{\| \bar{z}-\bar{E} \|^3} + \frac{M_m(\bar{z}-\bar{M})}{\| \bar{z}-\bar{M} \|^3}\right]. \quad (8)$$

The term $-w_1^2(1-\mu_s)L_S e^{i(\gamma_1-\gamma_2)}$ represents the centrifugal acceleration of B or, equivalently, the gravitational influence of the Sun on the Earth-Moon system, indeed (2) and (6) imply $(1-\mu_s)w_1^2 = \frac{GM_s}{L_S^3}$. The difference between (8) and

$$\frac{d^2\bar{z}}{d\tau^2} + 2iw_2\frac{d\bar{z}}{d\tau} - w_2^2\bar{z} = -G\left[\frac{M_e(\bar{z}-\bar{E})}{\| \bar{z}-\bar{E} \|^3} + \frac{M_m(\bar{z}-\bar{M})}{\| \bar{z}-\bar{M} \|^3}\right]$$

that describes the motion in the EM restricted problem, gives the distance between the two models

$$\Delta_{EM}(\bar{z}) = \| BCP - CR3BP_{EM} \| = GM_s\left|\left|\frac{(\bar{S}-\bar{z})}{\| \bar{z}-\bar{S} \|^3} - \frac{(\bar{S}-\bar{B})}{\| \bar{S}-\bar{B} \|^3}\right|\right|.$$

The error originates because in the CR3BP$_{EM}$ the influence of the Sun on the spacecraft is considered as the same influence that the Sun produces on the center B of the rotating frame. Indeed the error vanishes whenever the spacecraft is placed in the origin of the reference frame and grows when it moves away, see Fig. 3.

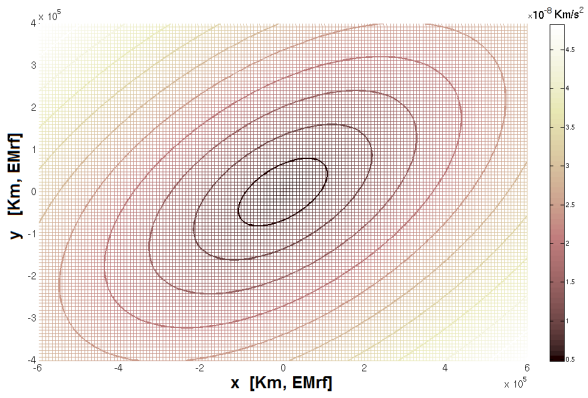

Fig. 3. Level curves of Δ_{EM} for $\theta = \pi/3$

3. REGIONS OF PREVALENCE

We investigate the prevalence of the CR3BPs according to which one produces the lowest error if it is considered in place of the BCP. To this aim, once a system of coordinates is chosen, let be defined the function

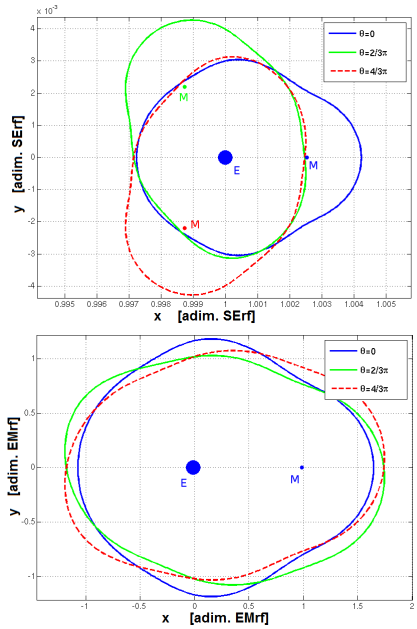

Fig. 4. $\Gamma(\theta)$ with $\theta = 0, 2/3\pi, 4/3\pi$ in SE and EM reference frame

$$\Delta E(z) = (\Delta_{SE} - \Delta_{EM})(z) = G\left|\left| -\frac{M_e(z-E)}{\| z-E \|^3} - \frac{M_m(z-M)}{\| z-M \|^3} + \frac{M_b(z-B)}{\| z-B \|^3}\right|\right| - GM_s\left|\left|\frac{(S-z)}{\| z-S \|^3} - \frac{(S-B)}{\| S-B \|^3}\right|\right|.$$

In any point z one of the restricted models as to be preferred according with the sign of ΔE: where $\Delta E < 0$ the CR3BP$_{SE}$ provides a better approximation of the BCP, otherwise the CR3BP$_{EM}$.

Denote with $\Gamma(\theta)$ the zero level set of the function ΔE for a given angle θ:

$$\Gamma(\theta) := \{z : \Delta E(z) = 0\}.$$

Numerical simulations show that $\Gamma(\theta)$ is a closed simple curve: we refer to the two regions bounded by $\Gamma(\theta)$ as the *Regions of Prevalence* of the two restricted problems. In the bounded region $\Delta_{EM} < \Delta_{SE}$, while in the exterior region the opposite holds. Substituting the coordinates giving the positions of the primaries, the zero level curve $\Gamma(\theta)$ is computed in SE and EM-synodical coordinates.

In Fig. 4 the zero level set of ΔE is drawn for different choices of the angle θ and in different system of coordinates. For any angle θ the Earth, the Moon as like as the L_1 and L_2 Lagrangian points related to the CR3BP$_{EM}$ belong to the EM region of prevalence, while the CR3BP$_{SE}$ Lagrangian points are placed in the exterior region.

4. THE COUPLED CR3BP APPROXIMATION

The coupled CR3BP concerns the approximation of the four-body problem with the superposition of two circular restricted three-body problems, (Koon et al. (2001)). Here the design of trajectories leaving a Lyapunov orbit around L_1 and L_2 in the CR3BP$_{SE}$ and directed to the vicinity of the Moon is considered: therefore, denoting with $W^{(u),s}_{(SE),EM,i}(\gamma)$ any (un)-stable manifold related to Lyapunov orbits γ around L_i in the (SE) or EM restricted

problem, the intersections of $W^s_{EM,2}(\gamma_1)$ with $W^u_{SE,1}(\gamma_2)$ and $W^u_{SE,2}(\gamma_2)$ have been exploited. According with the prevalence regions previously defined, the Poincaré section is set on the curve $\Gamma(\theta)$. The procedure to design the transfer trajectories is the following: first the angle θ is chosen and the curve $\Gamma(\theta)$ in both the synodical systems is set. After, for a couple of Lyapunov orbits γ_1, γ_2, the $W^s_{EM,2}(\gamma_1)$ and $W^u_{SE,1,2}(\gamma_2)$ are computed, each in their own coordinate frame, until the corresponding curve $\Gamma(\theta)$ is encountered. The resulting Poincaré map are then transformed into the same coordinates system and the connection point Int is selected.

As shown in Fig. 5, for almost every Lyapunov orbits around L_2 in the EM system and every θ, the external stable manifold $W^s_{EM,2}(\gamma_1)$ invests completely the curve $\Gamma(\theta)$: the resulting Poincaré map, topologically equivalent to a circle, bounds the region $\mathcal{B}$ of those initial data leading to the Moon's region.

For our purpose the point Int has to be selected in the set $\mathcal{B} \cap W^u_{SE,1,2}$. Patching together the trajectories obtained integrating the point Int backward in time in the CR3BP$_{SE}$ and forward in the CR3BP$_{EM}$, it follows an orbit that, starting from the SE-Lyapunov, after have passed through the EM Lyapunov gateway, will go close to the Moon.

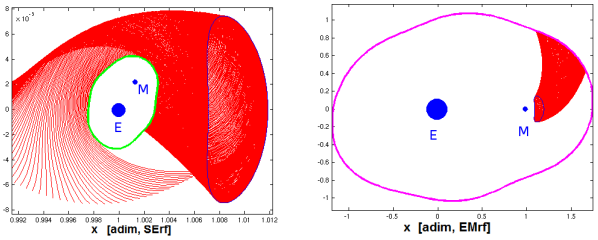

Fig. 5. Intersection of $W^u_{SE,2}(\gamma_2)$ and $W^s_{EM,2}(\gamma_1)$ with $\Gamma(\pi/3)$

5. THE BOX COVERING APPROACH

Using a software package called GAIO (Global Analysis of Invariant Objects), see Dellnitz et al. (2000), the four-dimensional Poincaré map is covered with box structures. A N-dimensional box $B(C,R)$ is identified by a center $C = (C_1, C_2, \ldots, C_N) \in \mathcal{R}^N$ and a vector of radii $R = (r_1, r_2, \ldots, r_N)$ and it is defined as

$$B(C,R) = \bigcap_{i=1}^{N} \{(x_1, x_2, \ldots, x_N) \in \mathcal{R}^N \ : \ |x_i - C_i| < r_i\}$$

Following a multiple subdivision process, starting from a box B_0, a larger family of smaller boxes is created with the property to cover B_0: the depth d of a family denotes the number of such subdivision iterations. Once the family $\mathcal{F}(d)$ of boxes is created, the Poincaré map is therein inserted: only those boxes of $\mathcal{F}(d)$ containing at least one point of the Poincaré map are considered, the others are neglected. Denote with $\mathcal{P}$ the family of boxes used for the covering of the Poincaré map. In order to detect the points Int, the interior region $\mathcal{B}$ needs to be covered as well, see Fig. 6. The definition of the centers of the boxes used to cover $\mathcal{B}$ is made 'by columns': from the set of boxes in $\mathcal{P}$ whose centers have the same (x,y)-coordinates, let be selected the two boxes with the maximal v_{max} and minimal v_{min} value of the v-coordinate. Then a new set of centers $\{C_k = (x, y, v_k, w_k)\}_{k=1}^{K}$ are defined, where $v_k = v_{min} + k\Delta v$ and w_k is obtained from the Jacobi constant. Here Δv is twice the radius in the v-direction of the covering boxes and $K = (v_{max} - v_{min})/\Delta v$.

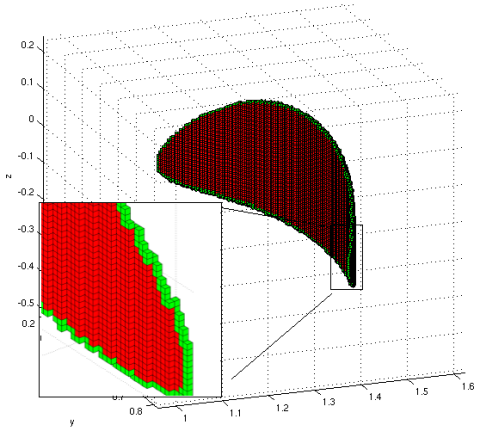

Fig. 6. Box covering of the interior region $\mathcal{B}$

In the presented simulation the covering is performed at $d = 32$: depending on the size of the Poincaré map the radii of the covering boxes result to be in the range $[4 \cdot 10^{-4}, 2 \cdot 10^{-3}]$ EM units.

Then, for a value of the Jacobi integral in the SE system, the Poincaré map of $W^u_{SE,1}(\gamma_2)$ or $W^u_{SE,2}(\gamma_2)$ is computed and, using (4), it is transformed in EM synodical coordinates, being θ the angle between the primaries. Finally, all those points of the SE Poincaré map lying in one of the boxes covering $\mathcal{B}$ are considered as transfer points.

6. SOME RESULTS

The existence of connection points is tested starting from a database of 60 Lyapunov orbits in the CR3BP$_{SE}$ both around L_1 and L_2 and 60 Lyapunov orbits around L_2 in the CR3BP$_{EM}$. The Jacobi constant varies in the range $[3.0004, 3.00084]$ for the SE system and in the interval $[3.053, 3.177]$ for the EM system and 32 values of θ have been considered.

Fig. 7 concerns transfers leaving a Lyapunov orbit around L_1: every dark sign marks a point in the intersection $\mathcal{B} \cap W^u_{SE,1}$, i.e. $\Delta V = 0$ connections. The coordinates represent the Jacobi constant of the connection point respectively in the SE and EM system and the angle θ of the Poincaré section $\Gamma(\theta)$ where the connection is detected. The lighter points are the projections of the previous ones onto the coordinates planes. Starting from one intersection, backward and forward integration in the two CR3BP produce the complete transfer. If no differently specified, all the evaluations are done in the SE-synodical frame and in SE-units of measure: relations 7 and 5 provide the accelerations of the spacecraft moving according to the Bicircular motion and CR3BP. In the following figures the darker and the lighter lines concern the pieces of trajectory integrated in the CR3BP$_{SE}$ and in the CR3BP$_{EM}$ respectively. In Fig. 8 the bigger picture depicts the orbit from a Lyapunov orbit around L_2 to the

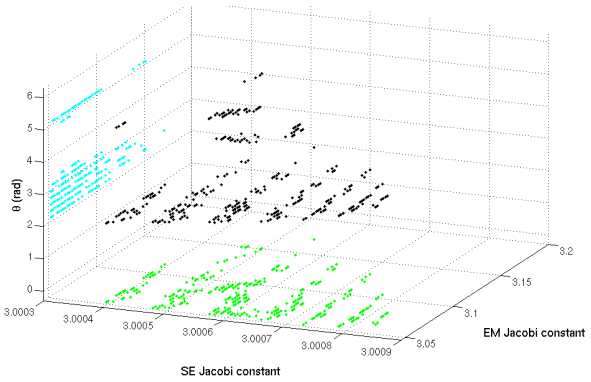

Fig. 7. Zero ΔV connections between $W^u_{SE,1}$ and $W^s_{EM,2}$

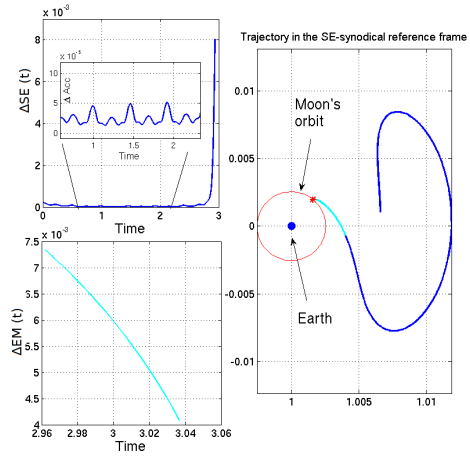

Fig. 8. Example of transfer trajectory and related errors Δ_{SE}, Δ_{EM}.

Moon region, while the smaller ones show the values of $\Delta_{SE}(t)$ and $\Delta_{EM}(t)$ evaluated along the trajectory.

The integral total $\Delta V = \int_{t_0}^{t_c} \Delta_{SE}(t)dt + \int_{t_c}^{t_{fin}} \Delta_{EM}(t)dt$ is used as a measure of the distance between the coupled model and the BCP. Here t_0 is the last time when the spacecraft is far from the Earth more than 2.5 times the Earth-Moon distance and t_{fin} is the first moment the spacecraft is 10000 km close to the Moon, while t_c denotes the instant when the Poincaré section is crossed. Referring to Fig. 9, in the bigger figure the dotted line remarks the circle inside which the above integration starts, the black circles show the position of the Moon when the spacecraft is on the section and at the end of the travel, the black line denotes the Poincaré section at the crossing time. In the upper of the smaller boxes the values of Δ_{EM} and Δ_{SE} are plotted together, while the last graph shows the value of the integration. Starting from t_0 the error Δ_{SE} is integrated until the crossing moment t_c, then two different integrations are done: in the first case the error Δ_{EM} is considered till the final time t_{fin} (lighter line), in the second case again Δ_{SE} is integrated for a short interval of time (darker line).

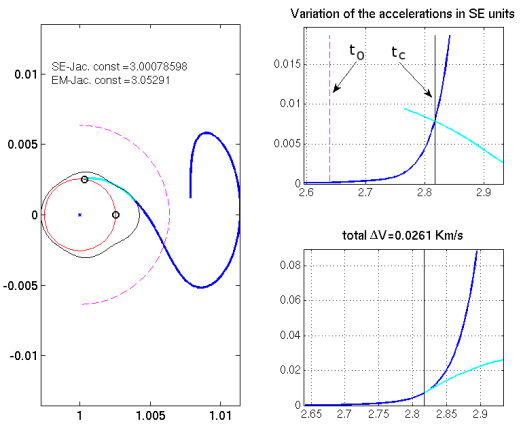

Fig. 9. Example of trajectory. Analysis of the error.

A more detailed analysis and a comparison with the trajectories designed adopting a classical Poincaré section will be given on a longer version of the present paper.

REFERENCES

E. Belbruno and J. Miller. Sun-perturbed Earth-to-Moon transfer with ballistic capture. *Journal of Guidance Control and Dynamics*, 16, 1993.

J. Cronin, P. B. Richards, and L. H. Russell. Some periodic solutions of a four-body problem. *Icarus*, 3(5-6):423 – 428, 1964.

M. Dellnitz, G. Froyland, and O. Junge. The algorithms behind GAIO - Set oriented numerical methods for dynamical systems. In *In Ergodic theory, analysis, and efficient simulation of dynamical systems*, pages 145–174. Springer, 2000.

M. Dellnitz, O. Junge, M. Post, and B. Thiere. On target for Venus – Set oriented computation of energy efficient low thrust trajectories. *Celestial Mech. Dynam. Astronom.*, 95(1-4):357–370, 2006.

G. Gómez, W.S. Koon, M.W. Lo, J.E. Marsden, J. Masdemont, and S.D. Ross. Connecting orbits and invariant manifolds in the spatial restricted three-body problem. *Nonlinearity*, 17:1571–1606, 2004.

W. S. Koon, M. W. Lo, J. E. Marsden, E. Jerrold, and S. D. Ross. Heteroclinic connections between periodic orbits and resonance transitions in celestial mechanics. *Chaos*, 10(2):427–469, 2000.

W. S. Koon, M. W. Lo, J. E. Marsden, and S. D. Ross. Low energy transfer to the Moon. *Celestial Mech. Dynam. Astronom.*, 81(1-2):63–73, 2001.

G. Mingotti, F.Topputo, and F. Bernelli-Zazzera. Low-energy, low-thrust transfers to the Moon. *Celestial Mech. Dynam. Astronom.*, 105(1-3):61–74, 2009.

J.S. Parker. Families of low-energy Lunar halo trasfer. *Proceedings of the AAS/AIAA Space Flight Mechanics Meeting*, pages 483–502, 2006.

C. Simó, G. Gómez, À Jorba, and J. Masdemont. The Bicircular model near the triangular libration points of the RTBP. In *From Newton to chaos*, volume 336 of *NATO Adv. Sci. Inst. Ser. B Phys.*, pages 343–370. 1995.

V. Szebehely. *Theory of orbits, the restricted problem of three bodies*. Academic Press, New York and London, 1967.

K. Yagasaki. Sun-perturbed Earth-to-Moon transfers with low energy and moderate flight time. *Celestial Mech. Dynam. Astronom.*, 90(3-4):197–212, 2004.